Original Research

Hyperglycemia results in significant pathophysiological changes of placental spiral artery remodeling and angiogenesis, further contributing to congenital defects

Yushu Qin[1,†], Naomi McCauley[1,†], Zehuan Ding[1,†], Lauren Lawless[1,2], Zhimin Liu[1,§], Ke Zhang[1,2], Linglin Xie[1,*]

[1]*Department of Nutrition, Texas A&M University, College Station, TX 77843, USA,* [2]*Center for Epigenetics & Disease Prevention, Institute of Biosciences & Technology, Texas A&M University, Houston, TX 77843, USA*

TABLE OF CONTENTS

1. Abstract

Introduction: Hyperglycemic conditions achieved during pregnancy have been shown to have detrimental effects to fetal development and increase the prevalence of childhood comorbidities. However, the mechanisms in which diabetic pregnancies affect placental development and subsequently contribute to adverse health effects on the mother and offspring remain unclear. **Research design and methods**: Streptozotocin was used to induce gestational diabetes in mice. In this model, hyperglycemia was established at embryonic day 3.5 (E3.5). Pregnancy mass was collected at E10.5, E12.5, E14.5, and E16.5 for different assessments. **Results**: Both placental and embryonic weights were found to be significantly elevated at E16.5. At E14.5, a significantly larger

Submitted: 4 September 2021 Revised: 18 October 2021 Accepted: 28 October 2021 Published: 30 November 2021

junctional zone with increased number of glycogen trophoblasts was found in the placentas from hyperglycemic pregnancies (HG group) compared to the placentas from normoglycemic pregnancies (NG group). Importantly, the HG placenta exhibited decreased trophoblast giant cell (TGC) association and TUNEL+ cells, and increased expression of α-SMA on the spiral artery, suggesting arterial remodeling was impacted. Moreover, the interhemal membrane of the labyrinth layer, was found to be thicker in the HG placentas. Furthermore, hyperglycemia resulted in more offspring congenital defects, which were associated with a thicker interhemal membrane. **Conclusions**: Together, these results suggest that gestational diabetes perturbs proper placental development and function, specifically spiral artery remodeling and angiogenesis, thereby negatively impacting embryonic development.

2. Introduction

Diabetes during pregnancy is known to affect the health of both mothers and their infants. Among the two types of diabetes during pregnancy, gestational diabetes (GDM) accounts for 90% and pre-gestational diabetes (PGDM) comprises the remaining 10% [1, 2]. In the United States, the GDM prevalence among pregnant women is as high as 9.2% [3]. With the introduction of insulin, diabetic-associated fetal mortality rates are reduced from 70% to nearly 12%. Unfortunately, the present birth defect rate in diabetic pregnancies (~10%) is still higher than that of the general population (3%), and appears to be ever increasing [2–6]. It has been suggested that placental damages from diabetic pregnancies could be the cause of fetal complications observed in the human population [7].

For a successful and healthy pregnancy, proper spiral artery (SpA) remodeling and labyrinth (LZ) angiogenesis are crucial for the establishment of adequate blood supply. Maternal blood is delivered to the placenta through the maternal SpAs, which reside in the endometrium of the uterus. During early stages of pregnancy, SpAs are classified as high resistance vessels and are surrounded by vascular smooth muscle cells (VSMCs). In order to provide adequate blood to the developing fetus, the maternal SpAs will undergo an invasive remodeling process, in which the VSMCs, possessing contractile properties, are replaced with invasive trophoblast cells [8], resulting in dilated and low resistance arteries [9]. As the intermediate barrier between fetal and maternal circulations, the placenta contains a highly developed blood network in the LZ layer. Different transporters are localized on the interhemal membrane (IHM), which separates the maternal and fetal blood. These establish a vascular network that will allow for the efficient exchange of nutrients and waste [8, 10, 11].

There is emerging evidence showing that placental malformation is a complication of diabetic pregnancies [12]. Hyperglycemic placentas are characterized by villous immaturity and edema, syncytial nodes, fibrin thrombus, and fibrinoid necrosis [7]. In addition, placentas from diabetic pregnancies have been reported to undergo “premature aging”, which is detected by early emergence of placental lobe calcifications [7]. All these problems disrupt placental vasculature and result in inefficient exchange of nutrients and waste [13]. Therefore, it has been speculated that transport efficiency can be impacted by a diabetic pregnancy. Additionally, shallow remodeling of spiral arteries have been observed under gestational diabetic and preeclamptic conditions [14, 15]. Despite the known pathological changes in hyperglycemic placentas, details of how this condition affects the process of SpA remodeling and angiogenesis remain unclear.

To gain a detailed insight into the pathology and underlying mechanisms of the placenta under hyperglycemic conditions, a streptozotocin (STZ)-induced hyperglycemic mouse model of pregnancy was employed. The pathological changes of the placenta due to hyperglycemia were evaluated, followed by experiments to investigate the underlying cellular and molecular mechanisms. Additionally, the incidences of several congenital birth defects, caused by the diabetic pregnancy, were also reported.

3. Methods

3.1 Chemicals, antibodies, and reagents

STZ (Cat#: S0130) was purchased from Sigma (Oakville, Ontario, Canada). Anti-αSMA rabbit antibody (Cat#: ab7817), anti-Cytokeratin18 mouse antibody (Cat#: ab668), anti-Tpbpα rabbit antibody (Cat#: ab104401) and anti-Histone H3 (phospho S10) (p-H3S10) antibody (Cat#: ab5176) were purchased from Abcam (Cambridge, UK). Anti-CD31 rabbit antibody (Cat#: 77699) was purchased from Cell Signaling Technology (Danvers, MA). DAPI mounting medium (Cat#: F6057) was purchased from Sigma (Oakville, Ontario, Canada).

3.2 Mouse model of gestational diabetes

Wildtype (*WT*), C57BL/6J female mice, between the ages of 8–11 weeks, were maintained with a chow diet (9% fat) and water *ad libitum* under a 12 h light/dark cycle throughout the experiment. Prior to treatment, mice body weights, basal blood glucose levels and age were recorded. The mice were then randomly selected and administered STZ, prepared in citrate buffer (pH 7.4), at a dose of 100 mg/kg body weight (HG), or citrate buffer only (NG) on day 1 and day 4, intraperitoneally (Fig. 1A). After the second injection, the female mice were mated with male mice (C57BL/6J) overnight, and the following day at noon was considered as embryonic day 0.5 (E0.5). Random blood glucoses were measured daily after the first injection to identify the initial onset of diabetic conditions. Maternal blood glucose levels higher than 200 mg/dL were defined as

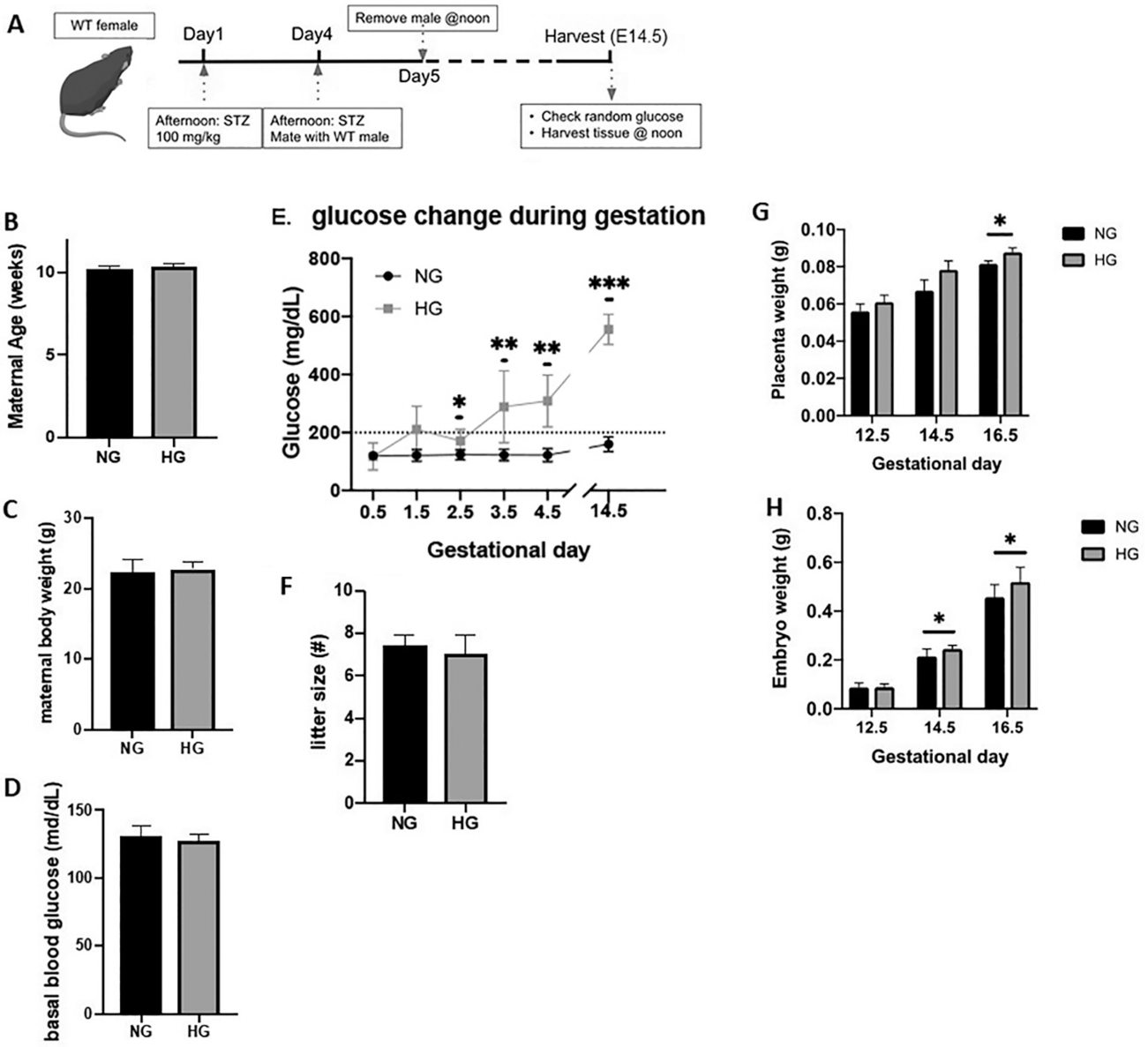

Fig. 1. STZ induced GDM results in larger placental and embryonic weight in later stages of pregnancy. (A) STZ treatment timeline. (B) Maternal age at start of treatment (NG n = 5; HG n = 10). (C) Maternal body weight at start of treatment (NG n = 5; HG n = 10). (D) Basal blood glucose at start of STZ treatment (NG n = 5; HG n = 10). (E) Maternal glucose level changes over time (NG n = 5; HG n = 10). (F) Litter size of samples collected at E14.5 (NG n = 5; HG n = 10). (G) Placenta weight changes over time (NG n = 5; HG n = 10). (H) Embryo weight changes over time (NG n = 5; HG n = 10). Data are presented as Mean ± SD.

a hyperglycemic pregnancy. Embryos and placentas were collected at E10.5, E12.5, E14.5 and E16.5.

All mouse experiments were completed according to a protocol reviewed and approved by the Institutional Animal Care and Use Committee of Texas A&M University, in compliance with the USA Public Health Service Policy on Humane Care and Use of Laboratory Animals.

3.3 Histology of mouse placenta

Placentas were sagittally bisected. Half of the placenta was stored at –80 °C, while the embryos and the remaining halves were fixed in 10% formalin at room temperature. The formalin fixed embryos and placentas were processed through an ethanol-xylene series and embedded in paraffin. 5 μm thick sections were collected. Routine procedures were used for H&E staining, periodic acid–Schiff (PAS) staining, immunohistochemical (IHC) staining and immunofluorescent (IF) staining. Isotype IgG was used for immunostaining negative control (**Supplementary Fig. 1**).

3.4 Spiral artery remodeling analysis

SpA remodeling during murine pregnancy involves the replacement of VSMCs by SpA-TGCs to form high circulation, low resistance blood vessels. A well-

Table 1. PCR primer sequences.

Acta2	GGCATCCACGAAACCACCTA	TTGCGTTCTGGAGGGGCAA
Mmp9	AGTTCTCTGGTGTGCCCTGG	GCAGGAGGTCGTAGGTCACG
Mmp14	CCCAAGGCAGCAACTTCAGC	GAGTGACTGGGGTGAGCGTT
Tgfb	TCGCTTTGTACAACAGCACC	ACTGCTTCCCGAATGTCTGA

remodeled SpA is surrounded by SpA-TGCs, with a dilated lumen to support an increased blood volume during pregnancy. The remodeling process was assessed by the level of TGCs associated with the SpAs at E14.5. Based on the percentage of the arterial wall surrounded by TGCs (Cytokeratin 18 (Cytok) positive), all observed SpAs were categorized as either unremodeled (0–25%), partially remodeled (25–75%), or remodeled (75–100%). Based on the ratio of the remodeled SpAs of each placenta, placentas were further classified as "TGC-associated" if more than 50% of the spiral arteries were remodeled or "TGC-unassociated" if less than 50% of the spiral arteries were remodeled. In addition, the lumen diameter (LD) to outer diameter (OD) ratio of the SpA was measured to determine the lumen size of the SpA.

RT-PCR was performed to measure the mRNA expression of TGC migration markers.

3.5 Fetal capillary area (FCA), maternal lacune area (MLA) and IHM thickness

The LZ angiogenesis was assessed by measuring the area of the maternal lacunae space, traced by Cytok expression, and the fetal blood space, labeled by CD31 positive staining, at both E14.5 and E16.5. Images of the LZ from CD31 and Cytok co-IF staining were captured with a Leica confocal microscope. In each sample, outlines of fetal capillary and maternal lacune areas in 10,000 μm^2 of the LZ layer were drawn based on CD31 staining (green) and Cytok staining (red), respectively, and the total areas were measured. The barrier between the fetal and maternal circulations, composed of endothelial cells, syncytiotrophoblasts and sinusoidal trophoblast giant cells, is defined as the IHM, and is an important structure for efficient nutrient and gas exchange [16]. To investigate placental nutrient transportation capacity, the IHM thickness was measured. Ten IHMs were randomly selected in each picture and the thinnest portion of the membrane between the fetal capillary and maternal lacunae was measured. All analyses were performed with ImageJ.

3.6 Western blot

The total protein from the placentas was extracted using Cell Lysis buffer (Cell Signaling Technology, Cat#: 9803). The concentrations were measured using the Pierce™ BCA Protein Assay Kit (Thermo Fisher Scientific, Cat#: 23225). 15–30 μg proteins were loaded on 7–12% SDS-PAGE electrophoresis gels and transferred onto PVDF membranes (Fisher Scientific, Hampton, NH, Cat#: 45-004-110). The membranes were then blocked with 5% fat-free milk, and incubated in the primary antibodies overnight at 4 °C. After incubation with the anti-rabbit secondary antibody (Cell Signaling Technology, Cat#: 7040) for 1 h, the signal was detected with the HRP substrate, and analyzed with the ImageJ.

3.7 Realtime-qPCR

The total RNA of mouse placentas was extracted using Trizol and RNA spin columns. cDNA was then synthesized using the SuperScript III Reverse Transcriptase kit (Thermo Fisher, Waltham, MA, Cat#: 18080051). RT-PCR was performed using a SYBR Green PCR master mix (Bio-Rad). Results were analyzed using the comparative C (T) method. The primers are listed in Table 1.

3.8 Statistical analysis

Embryos and placentas from at least 5 female mice per group were analyzed in this study. Data was analyzed by the student's *t*-test, Chi-square test, or one-way ANOVA. Results were considered significant when the *p* values were less than 0.05. All statistical analyses were carried out using GraphPad Prism.

4. Results

4.1 STZ injection induced hyperglycemia at E3.5

Before pregnancy, female mice demonstrated synonymous age and body weight (Fig. 1B,C). The blood glucose of the HG and NG groups were normal (Fig. 1D). Daily random blood glucose checks identified a significant increase of blood glucose levels in the HG group beginning at E2.5. At E3.5, 80% (8 out of 10) of the HG mice reached a hyperglycemic condition (>200 mg/dL), displaying blood glucose levels of 289 $\pm$ 123.9 mg/dL. By E4.5, all of the HG mice had obtained this hyperglycemic condition, which persisted throughout the pregnancy. At E14.5, the blood glucose levels of the HG group were as high as 555.7 $\pm$ 32.2 mg/dL, while the NG group remained at 160.3 $\pm$ 15.6 mg/dL (Fig. 1E). To be noted, the hyperglycemic status did not affect the litter size in this study (Fig. 1F).

4.2 Hyperglycemia increased placental and embryonic weights

Increased placental weights were observed in the HG group beginning at E12.5 and reached significance at E16.5 (Fig. 1G). The HG group also showed a significantly larger embryonic weight at E14.5 and E16.5 (Fig. 1H). The placental efficiency of the HG placentas was

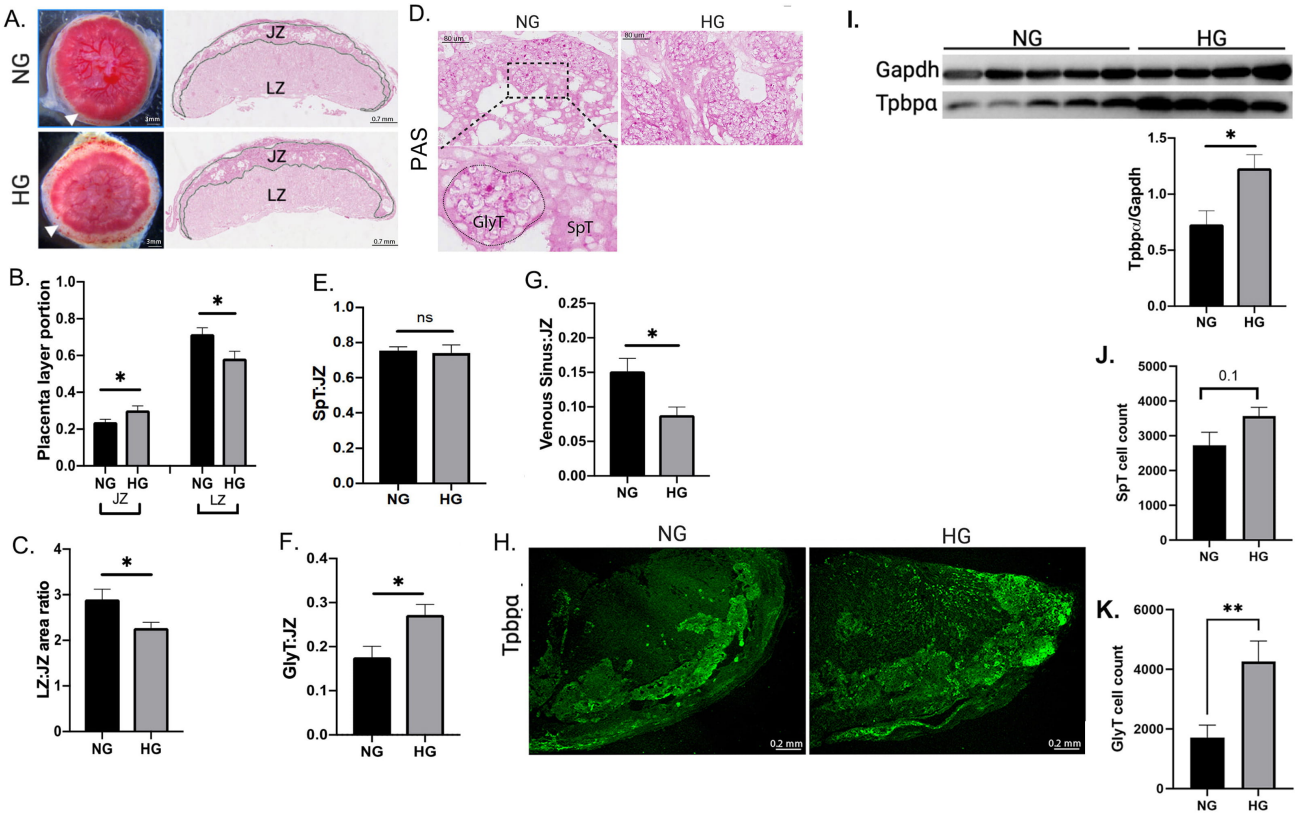

Fig. 2. E14.5 GDM placentas have larger JZ areas with increased GlyTs. (A) JZ visibly occupies a larger area of the placenta. Slide image from PAS staining. (B) JZ and LZ area proportion within the placenta (NG n = 8; HG n = 9). (C) LZ to JZ ratio (NG n = 8; HG n = 9). (D) PAS staining of GlyTs within the JZ and IF staining of Tpbpα. (E) Area proportion of JZ occupied by SpTs (NG n = 9; HG n = 10). (F) Area proportion of JZ occupied by GlyTs (NG n = 9; HG n = 10). (G) Area proportion of JZ occupied by venous sinuses (NG n = 9; HG n = 9). (H) Tpbpα protein expression localization in placenta. (I) Tpbpα protein expression level in whole placenta lysate. (J) Numbers of SpT cell in the entire JZ (NG n = 5; HG n = 5). (K) Numbers of GlyT cell in the entire JZ (NG n = 5; HG n = 5). Data are presented as Mean ± SD.

lower at E12.5, but this observation was reversed at E16.5 (**Supplementary Fig. 1**).

4.3 Hyperglycemia increased the percentage of glycogen trophoblast (GlyT) cells in the JZ

The effect of GDM on placenta morphology was assessed at E14.5. An increased thickness in the junctional zone (JZ) was observed in the HG placentas (Fig. 2A, white arrow). Additionally, the HG placenta displayed a larger portion of the whole placenta to be occupied by the JZ and the LZ to take up a smaller portion, when compared to the NG placenta (Fig. 2B). This resulted in a significantly smaller LZ to JZ area ratio in HG placentas (Fig. 2C). PAS staining was performed to specifically label the glycogen trophoblast cells (GlyTs), which are enriched with glycogen (Fig. 2D). Thus, the PAS negative cell population was majorly composed of spongiotrophoblast cells (SpTs). The PAS staining showed no difference in the SpT area ratios in the JZ area of the HG and NG groups. However, a larger ratio of GlyT area was noticed in the HG group (Fig. 2F). In addition, the total area of the venous sinus was significantly decreased in the JZ of the HG group (Fig. 2G). Tpbpα staining (Fig. 2H) showed that the number of SpTs is not changed, while the GlyT cell count increased significantly (Fig. 2J,K). Western blots performed on the whole placenta showed that hyperglycemia enhanced the level of Tpbpα (Fig. 2I), a protein highly expressed in GlyT, which is consistent with the increased total area of GlyTs.

4.4 SpA remodeling is compromised under hyperglycemia

The decidua (DZ) layer was found to have fewer TGCs, marked by Cytok expression (Cytok+), surrounding the SpAs (CD31+) in the HG placentas (Fig. 3A). When all TGC associations to SpAs were evaluated together, the HG placenta presented more unremodeled SpAs, and less partially and fully remodeled SpAs (Fig. 3B). As shown in Table 2, 9 out of the 10 NG placentas were graded as “TGC-associated”, while the HG group only had 3 out of 9 TGC-associated placentas. The placentas from the HG group also had a significantly smaller LD/OD ratio (Fig. 3C,D). The SpA remodeling level was further evaluated by the expression of α-SMA, a marker of VSMCs that surround the SpA. The HG placenta showed a higher α-SMA expression on the SpA (Fig. 3E), and less apoptotic cells surrounding the SpAs (Fig. 3F), suggesting hindered remodeling. Consis-

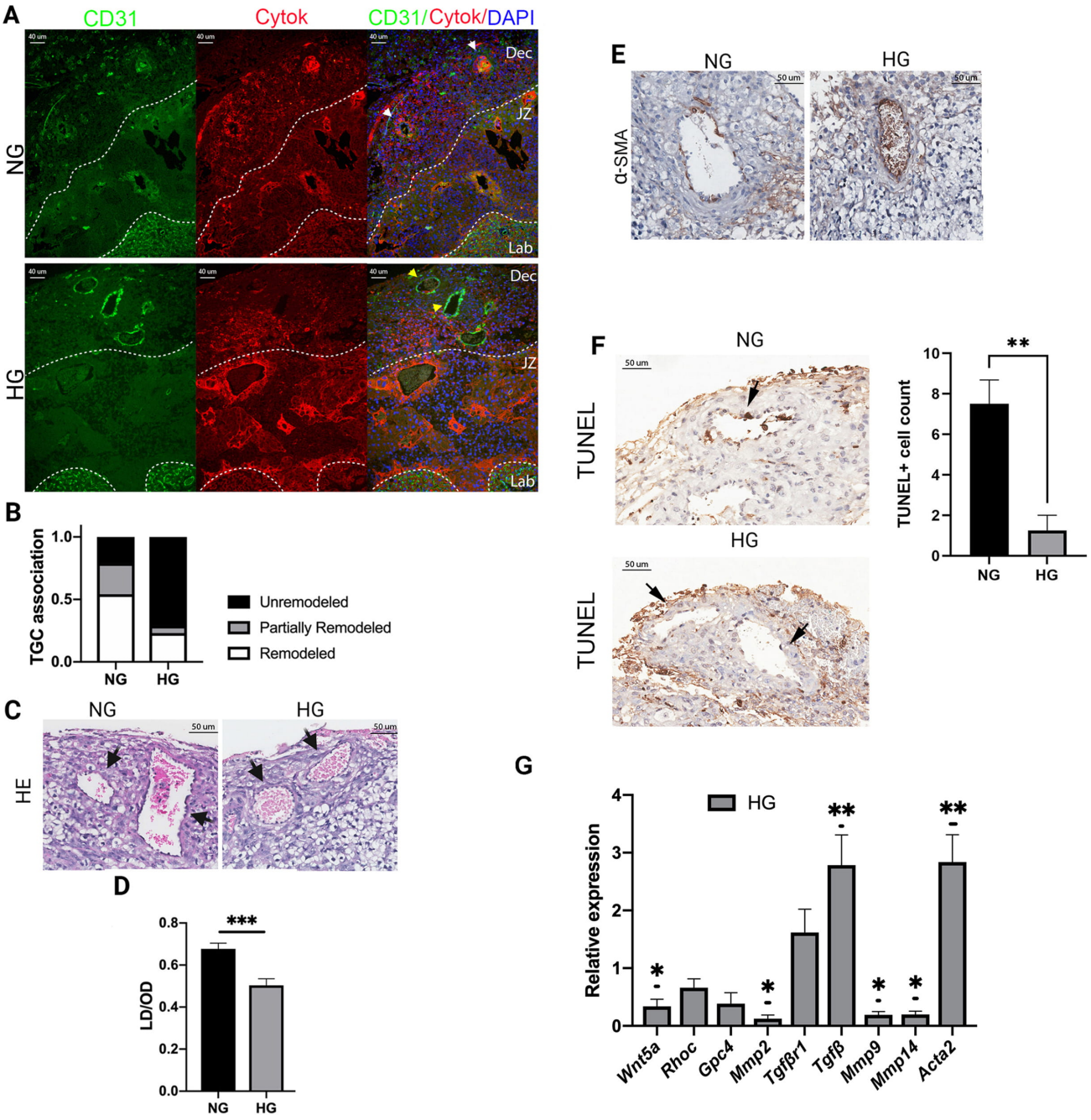

Fig. 3. GDM hinders SpA remodeling evidenced by decreased TGC association, VSMC breakdown, and mRNA expression of migratory genes. (A) Co-IF of CD31, Cytok, and DAPI. SpAs and TGCs are visualized by CD31 and Cytok, respectively. (B) Ratio of classification of TGC association by sample (NG n = 9; HG n = 10). (C) Vascular wall structure visualized by H&E staining. (D) LD to OD ratio indicating degree of vascular remodeling (NG n = 10; HG n = 10). (E) SpA VSMC visualized by α-SMA IHC. (F) TUNEL staining on SpA. SpA indicated by the black arrow. #TUNEL+ cell around the SpA (NG n = 5; HG n = 5). (G) mRNA level of genes involved in TGC migration and SpA vascular wall composition at E12.5 (NG n = 4; HG n = 4). Data are presented as Mean ± SD.

tently, the mRNA expression level of *Acta2*, which is an alias for *α*-SMA [17], was found to be significantly higher in the HG placentas at E12.5 (Fig. 3G), suggesting an increased presence of VSMCs, hence decreased remodeling by TGCs.

The reduced number of SpA-TGCs and discrepancies observed in the SpA wall suggested a migration problem of the TGCs. Thus, the influence of GDM on the expression of genes involved in TGC migration was then examined. Mmp2, Mmp9 and Mmp14 are pro-migratory proteins, while *Tgfβ* is anti-migratory [10, 18]. *Wnt5a is known to induce cell migration* [19, 20]. A significant decrease in

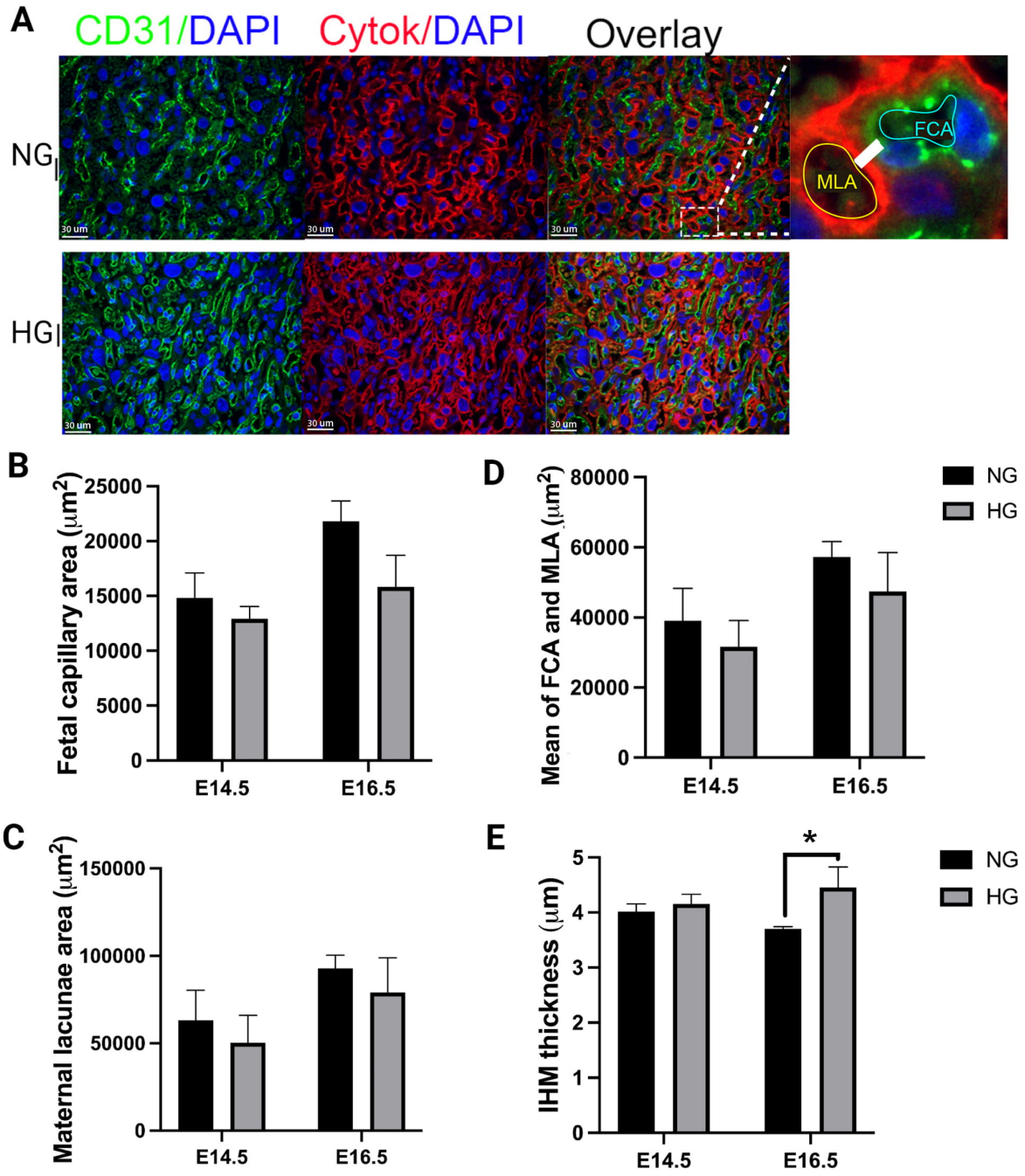

Fig. 4. GDM increases IHM thickness. (A) Co-IF of CD31, Cytok, and DAPI. Zoomed in example shows the IHM (white bar), MLA (yellow line) and FCA (cyan line) that was measured for (B) (C) (E). (B) FCA defined by area enclosed by CD31 (NG n = 7; HG n = 7). (C) MLA defined by area encircled by Cytok and not occupied by fetal capillary or DAPI (NG n = 7; HG n = 7). (D) Mean of FCA and MLA (NG n = 7; HG n = 7). (E) IHM thickness (NG n = 7; HG n = 7). Data are presented as Mean ± SD.

Mmp2, *Mmp9*, *Mmp14*, *and Wnt5a* mRNA transcripts, and an increase in the *Tgfβ* levels were observed in the HG placentas (Fig. 3G).

4.5 Hyperglycemia increases the IHM thickness

The HG group had a decreased trend of fetal blood space and the maternal lacunae area at both E14.5 and E16.5, however neither showed statistical significance (Fig. 4A–C). The mean of the maternal lacunae and fetal capillary space also did not show any differences between the HG and NG groups (Fig. 4D). The HG placentas were found to display a thicker IHM compared to the NG placentas at E16.5 (Fig. 4E).

4.6 GDM causes congenital malformations and hyperplastic ventricular disease

To gain an insight of how hyperglycemia impacts embryonic development, embryos were harvested at E14.5.

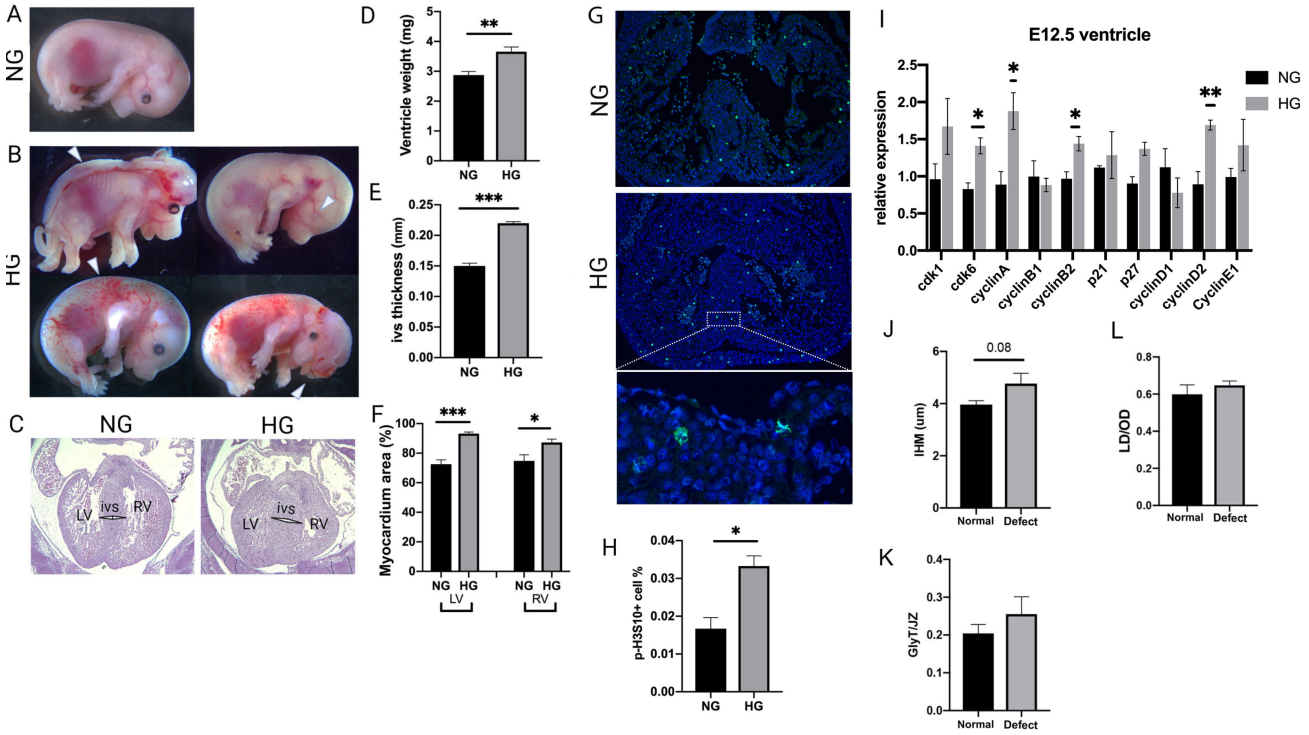

Fig. 5. GDM increases the incidence of hyperplastic ventricular disease and congenital malformations. IHM thickness is increased in placentas from malformed embryos. (A) Normal embryo at E14.5. (B) Observed congenital malformations include NTD, ocular defect, craniofacial defect, and edema. (C) H&E staining of E14.5 embryonic hearts labeled with LV, RV, and IVS. (D) Heart weight (NG n = 7; HG n = 7). (E) IVS thickness (NG n = 4; HG n = 4). (F) Myocardium tissue area that occupies the left and right ventricle individually (NG n = 10; HG n = 10). (G) p-H3S10 IF staining of heart sections at E12.5. (H) p-H3S10 positive cell percentage at E12.5 (NG n = 4; HG n = 4). (I) mRNA level of genes involved in cell cycle and proliferation at E12.5 (NG n = 4; HG n = 4). (J) IHM thickness in placenta from normal embryos and embryos with congenital defects (NG n = 5; HG n = 3). (K) GlyT/SpT ratio in placenta from normal embryos and embryos with congenital defects (NG n = 5; HG n = 3). (L) SpA LD/OD ratio in placenta from normal and congenital defect embryos (NG n = 5; HG n = 3). Data are presented as Mean ± SD.

Table 2. TGC-association level on SpA.

	Total	Associated	Unassociated
NG	10	9	1
HG	9	3	6
p-value*		0.02	

* The *p*-value was calculated via χ^2 tests.

The number of congenital defects, including the neural tube defects (NTD), ocular defects, craniofacial defects, and heart defects, were counted (Fig. 5A,B). 11 out of 73 of the HG embryos displayed at least one type of the evaluated birth defects, while no birth defects were observed in the NG group (Table 3, $p < 0.001$ by Chi-square test). These congenital defects included 6 cases of NTDs, 3 cases of ocular defects and 1 case of a craniofacial defect (Fig. 5A,B). Statistically, the HG group had significantly more incidences of NTDs than the NG group (Table 3, $p < 0.01$ by Chi-square test). The incidence of heart defects, including atrial septum defects, ventricular septum defects and outflow tract defects, was not different between the HG and NG groups, according to the examination of 7 NG and 17 HG hearts randomly selected (Table 4, 1/17 vs 0/7, $p >$ 0.05). Edema was also observed in 2 out of 73 HG embryos, showing no statistical difference from the NG group (Table 3). Embryonic hearts were further examined for the interventricular septum (IVS) thickness and the presence of cardiac hypertrophy or hyperplasia. Overall, dense ventricles and increased ventricular weight of the embryonic heart were observed in the HG group compared to the NG group (Fig. 5C,D). Specifically, a thicker IVS was observed in the HG embryo (Fig. 5C,E). The HG embryonic heart also had an increased myocardial area of both the left and right ventricle (Fig. 5C,F). IF staining of p-H3S10 was performed on heart sections at E12.5 to determine if proliferation of ventricular cardiomyocytes was affected by hyperglycemia. A significant increase in the percentage of proliferating cardiomyocytes, labeled by p-H3S10 expression, was found in the HG group, when compared to the NG group (Fig. 5G,H). A significant increase in *Cdk6*, *Cyclin A*, *Cyclin B2* and *Cyclin D2* mRNA transcripts was observed in the HG heart ventricle (Fig. 5I). These results suggested cardiac hyperplasia in the HG embryos.

Table 3. Number of congenital defects observed in GDM embryos increased*.

	Total	Normal	Total congenital defect	NTD	Ocular defect	Craniofacial defect
NG	81	81	0	0	0	0
HG	73	62	11	7	3	1
p-value*			$p < 0.001$ (0.0002)	$p < 0.01$ (0.0046)	0.104	0.474

* The *p*-values were calculated via the Fisher-Exact tests.

Table 4. Rate of cardiac structural defects was not affected by GDM.

	Total	ASD	VSD	DORV	OA
NG	7	0	0	0	0
HG	17	0	0	1	0

4.7 The IHM thickness was marginally increased in the placentas from embryos with congenital defects

To understand if the congenital birth defects were associated with any abnormal feature of the placenta, placental samples with congenital defects, regardless of them being in the NG or HG group, were pooled in a "Congenital Defect" group, while the rest were grouped as "Normal". One-way ANOVA was performed on the data of GlyT/SpT ratio, the LD/OD ratio and the IHM thickness. A Chi-square test was performed on the TGC-SpA association data in terms of congenital defect group versus the normal group. The results showed a marginal significance of IHM thickness and the congenital defects (p = 0.085), but not for the GlyT/SpT ratio (p = 0.200), the LD/OD ratio (p = 0.207) and the TGC-SpA association (p = 0.222) (Fig. 5J–L).

5. Discussion

In this study, the pathological changes of the placenta and its association with birth defects caused by hyperglycemia was investigated using a diabetic pregnant mouse model. Compared to other mouse studies that generated hyperglycemia before mating [21–23], this study utilized a mouse model with hyperglycemia established at E3.5. Pre-pregnancy diabetes has been known to affect ovulation and implantation [5]. Therefore, this model avoids placental abnormalities associated with pregnancy establishment. Embryos and placentas from hyperglycemic pregnancies were reported to have altered growth metrics. Additionally, placentas under hyperglycemic conditions were found to have a proportionately larger JZ, mainly due to an increased number of GlyTs. Most important, the hyperglycemic placentas displayed defects in SpA remodeling and IHM thickness. Interestingly, IHM thickness appeared to be associated with a higher incidence of birth defects in the embryos.

This study provides *in vivo* evidence of hyperglycemia disrupting SpA remodeling. This is indicated by decreased TGC association and higher remnants of αSMA on the vascular wall. These results suggest two potential mechanisms leading to hindered SpA remodeling. Firstly, migration alterations of the TGCs delays the process of TGCs replacing the VSMCs. Nteeba *et al.* [24] reported that STZ-induced hyperglycemic rat placentas had decreased interstitial trophoblast migration into the metrial gland. Consistent with this report, this study showed that hyperglycemic placentas had reduced *Mmp2*, *Mmp9* and *Mmp14* mRNA levels and increased *Tgfβ* mRNA levels, suggesting an inhibition of migratory signaling. Secondly, inhibition of VSMC apoptosis complicates the ability of the TGCs to replace the VSMCs. Through TUNEL staining, a decrease in VSMC apoptosis in HG placentas was observed. Indeed, decreased placental growth factor (PIGF) and uPA activation were observed previously in diabetic placentas, suggesting a potential decrease in apoptosis during SpA remodeling [25–27]. Furthermore, defective SpA remodeling has been suggested to result in blood pressure changes [28–31]. In humans, up to 50% of diabetic pregnancies were reported to develop pregnancy-induced hypertension [29–31]. Thus, GDM is considered a major risk factor for preeclampsia. Not only did our mouse GDM model reveal that SpA remodeling was hindered, but also showed a decrease in JZ venous sinus area. There are currently no studies to our knowledge that have examined the physiological consequences of decreased venous sinus in the placenta. However, in the brain, decreased venous sinus causes reduced venous flow, resulting in pressure buildup [32]. Taken together, this data provides a potential pathophysiological link of GDM and the etiology of preeclampsia.

LZ layer angiogenesis is critical for establishing proper blood supply to support a healthy pregnancy. Phenotypic analyses revealed that the IHM was thicker in the hyperglycemic group, consistent with observed thickening of the basement membrane in human GDM placentas [7, 33]. The cause of the thickened IHM is still unclear. One potential mechanism of this phenomenon is an extracellular matrix buildup due to an altered microenvironment accompanying inflammation [34]. It is also possible that premature trophoblasts observed in GDM placentas may alter the thickness of their cell membranes, which further affects the IHM [35, 36]. Additionally, human GDM placentas often show hypervascularization and villous immaturity [37]. However, these phenotypes were not observed in this murine study. A previous review suggested that GDM affects placental angiogenesis in later stages of pregnancy [38]. Therefore, future studies using later stages of placen-

tal development, e.g., E16.5 or E18.5, may elucidate the mechanisms behind hyperglycemic induced temporal dysregulation of placental angiogenesis.

It is suggested that the JZ is the most sensitive placental compartment to diabetic conditions [39–42]. Consistent with previous reports [40], hyperglycemic conditions caused the relative size of the JZ to increase in this study. The Tpbpα IF staining showed that the larger JZ area was mainly due to increased GlyTs and not SpTs. It has previously been reported that hyperglycemia enhances expression of genes involved in JZ development, such as *Taf7l*, *Pappa2*, and *Plac1* in the rat placenta [24]. Together, this data, along with other reports, suggest that hyperglycemia impacts the JZ development, particularly the cell population of this layer.

The mouse hyperglycemic pregnancies displayed an increased embryonic weight over time. Human GDM pregnancies are often complicated by macrosomia due to accelerated fetal growth in the later pregnancy [43]. In this GDM mouse model, a similar phenotype was observed, in which embryonic weight began to increase at E14.5 and was significantly higher at E16.5. Among the embryos that were collected at E14.5, the rate of congenital malformations, especially the NTDs, was increased in hyperglycemic pregnancies, which is a consistent finding in fetuses of diabetic pregnancies [44, 45]. In this study, congenital heart defects were not associated with diabetic pregnancies, which seems to be inconsistent with previous reports in humans [46]. This could be due to a small sample size not producing enough power for this association study, since the incidence rate of congenital heart defects in diabetic pregnancy was around 3% [47, 48]. However, hyperplastic ventricles due to increased cell proliferation, with a thickened IVS were observed in our hyperglycemic pregnant mouse model, which was consistent with other reports [45, 49]. It has been suggested that placental damages from GDM could be the cause of fetal complications observed in the human population [7]. Moreover, for the first time, this study demonstrated an association between IHM thickness and birth defects, although the same was not observed with GlyT/JZ nor LD/OD. The IHM is where exchange of gas and nutrients occur via diffusion, transporters, and endocytosis/exocytosis [50]. Theoretically, the transport of nutrients, such as sugars, amino acids, and fatty acids, will be affected when its travel distance across the maternal and fetal interface is relatively longer, as the IHM remains thicker under hyperglycemia. This altered availability, either in rate or amount, of these macro-nutrients during development could have an impact on crucial developmental milestones. Further research is needed to confirm this hypothesis.

6. Conclusions

In summary, we demonstrated that hyperglycemia disrupted SpA remodeling possibly via interference of SpA-TGCs migration. Placentas from hyperglycemic pregnancies had thickened IHM, which was associated with increased birth defects. This study provides insights into the placental changes that occur under hyperglycemic pregnancies *in vivo*. These observed morphological and molecular changes should be further explored to identify more focused targets affected by hyperglycemia to establish strategies to mitigate congenital malformations and pregnancy complications associated with GDM.

7. Author contributions

LX conceived the idea and designed the study; YQ, NM, ZD and ZL performed the experiments; KZ, YQ, NM, ZD and LL analyzed the data; LX, YQ, NM, ZD and LL wrote the manuscript.

8. Ethics approval and consent to participate

All mouse experiments were completed according to a protocol (AUP#2018-0309) reviewed and approved by the Institutional Animal Care and Use Committee of Texas A&M University, in compliance with the USA Public Health Service Policy on Humane Care and Use of Laboratory Animals.

9. Acknowledgment

Thanks to all the peer reviewers for their opinions and suggestions.

10. Funding

This project was supported by grants from the National Institutes of Health (NIDDK 1R01DK112368-01 to Drs. Xie and Zhang). This work was funded, in part, by the grant from the National Institute of Environmental Health Sciences (P30 ES029067).

11. Conflict of interest

The authors declare no conflict of interest.

12. In-house submissions

Given her role as Guest Editor in special issue: *The Effects of Maternal Nutrition on Metabolism of Infants and Children*, LX had no involvement in the peer-review of this article and has no access to information regarding its peer-review. Full responsibility for the editorial process for this article was delegated to GP.

13. References

[1] U.S. Preventive Services Task Force (USPSTF). Screening for gestational diabetes mellitus: recommendation and rationale. American Family Physician. 2003; 68: 331–335.

[2] Hami J, Shojae F, Vafaee-Nezhad S, Lotfi N, Kheradmand H, Haghir H. Some of the experimental and clinical aspects of the effects of the maternal diabetes on developing hippocampus. World Journal of Diabetes. 2015; 6: 412–422.

[3] DeSisto CL, Kim SY, Sharma AJ. Prevalence estimates of gestational diabetes mellitus in the United States, Pregnancy Risk Assessment Monitoring System (PRAMS), 2007–2010. Preventing Chronic Disease. 2014; 11: E104.

[4] Bánhidy F, Acs N, Puhó EH, Czeizel AE. Congenital abnormalities in the offspring of pregnant women with type 1, type 2 and gestational diabetes mellitus: a population-based case-control study. Congenital Anomalies. 2010; 50: 115–121.

[5] Ornoy A, Reece EA, Pavlinkova G, Kappen C, Miller RK. Effect of maternal diabetes on the embryo, fetus, and children: Congenital anomalies, genetic and epigenetic changes and developmental outcomes. Birth Defects Research Part C: Embryo Today: Reviews. 2015; 105: 53–72.

[6] Persson M, Cnattingius S, Villamor E, Söderling J, Pasternak B, Stephansson O, *et al*. Risk of major congenital malformations in relation to maternal overweight and obesity severity: cohort study of 1.2 million singletons. British Medical Journal. 2017; 357: j2563.

[7] Edu A, Teodorescu C, Dobjanschi CG, Socol ZZ, Teodorescu V, Matei A, *et al*. Placenta changes in pregnancy with gestational diabetes. Romanian Journal of Morphology and Embryology. 2016; 57: 507–512.

[8] Woods L, Perez-Garcia V, Hemberger M. Regulation of Placental Development and Its Impact on Fetal Growth-New Insights From Mouse Models. Frontiers in Endocrinology. 2018; 9: 570.

[9] Whitley GSJ, Cartwright JE. Cellular and Molecular Regulation of Spiral Artery Remodelling: Lessons from the Cardiovascular Field. Placenta. 2010; 31: 465–474.

[10] Pereira RD, De Long NE, Wang RC, Yazdi FT, Holloway AC, Raha S. Angiogenesis in the placenta: the role of reactive oxygen species signaling. BioMed Research International. 2015; 2015: 814543.

[11] Chen D, Zheng J. Regulation of Placental Angiogenesis. Microcirculation. 2014; 21: 15–25.

[12] Vambergue A, Fajardy I. Consequences of gestational and pregestational diabetes on placental function and birth weight. World Journal of Diabetes. 2011; 2: 196–203.

[13] Košir Pogačnik R, Trojner Bregar A, Lučovnik M, Krajec M, Verdenik I, Blickstein I, *et al*. The effect of interaction between parity, gestational diabetes, and pregravid obesity on the incidence of preeclampsia. The Journal of Maternal-Fetal & Neonatal Medicine. 2020; 33: 931–934.

[14] Desoye G. The Human Placenta in Diabetes and Obesity: Friend or Foe? The 2017 Norbert Freinkel Award Lecture. Diabetes Care. 2018; 41: 1362–1369.

[15] Staff AC. The two-stage placental model of preeclampsia: an update. Journal of Reproductive Immunology. 2019; 134-135: 1–10.

[16] Coan PM, Ferguson-Smith AC, Burton GJ. Developmental dynamics of the definitive mouse placenta assessed by stereology. Biology of Reproduction. 2004; 70: 1806–1813.

[17] Yuan S. A-Smooth Muscle Actin and ACTA2 Gene Expressions in Vasculopathies. Brazilian Journal of Cardiovascular Surgery. 2015; 30: 644–649.

[18] Schumacher A, Sharkey DJ, Robertson SA, Zenclussen AC. Immune Cells at the Fetomaternal Interface: how the Microenvironment Modulates Immune Cells to Foster Fetal Development. Journal of Immunology. 2018; 201: 325–334.

[19] He F, Xiong W, Yu X, Espinoza-Lewis R, Liu C, Gu S, *et al*. Wnt5a regulates directional cell migration and cell proliferation via Ror2-mediated noncanonical pathway in mammalian palate development. Development. 2008; 135: 3871–3879.

[20] Nishita M, Yoo SK, Nomachi A, Kani S, Sougawa N, Ohta Y, *et al*. Filopodia formation mediated by receptor tyrosine kinase Ror2 is required for Wnt5a-induced cell migration. The Journal of Cell Biology. 2006; 175: 555–562.

[21] Gül M, Bayat N, Çetin A, Kepekçi RA, Şimşek Y, Kayhan B, *et al*. Histopathological, Ultrastructural and Apoptotic Changes in Diabetic Rat Placenta. Balkan Medical Journal. 2015; 32: 296–302.

[22] Usman UZ, Bakar ABA, Mohamed M. Propolis improves pregnancy outcomes and placental oxidative stress status in streptozotocin-induced diabetic rats. BMC Complementary and Alternative Medicine. 2018; 18: 324.

[23] Wu J, Yan L. Streptozotocin-induced type 1 diabetes in rodents as a model for studying mitochondrial mechanisms of diabetic β cell glucotoxicity. Diabetes, Metabolic Syndrome and Obesity. 2015; 8: 181–188.

[24] Nteeba J, Varberg KM, Scott RL, Simon ME, Iqbal K, Soares MJ. Poorly controlled diabetes mellitus alters placental structure, efficiency, and plasticity. BMJ Open Diabetes Research & Care. 2020; 8: e001243.

[25] Heim KR, Mulla MJ, Potter JA, Han CS, Guller S, Abrahams VM. Excess glucose induce trophoblast inflammation and limit cell migration through HMGB1 activation of Toll-Like receptor 4. American Journal of Reproductive Immunology. 2018; 80: e13044.

[26] Tao J, Xia L, Chen J, Zeng J, Meng J, Wu S, *et al*. High glucose condition inhibits trophoblast proliferation, migration and invasion by downregulating placental growth factor expression. Journal of Obstetrics and Gynaecology Research. 2020; 46: 1690–1701.

[27] Belkacemi L, Lash GE, Macdonald-Goodfellow SK, Caldwell JD, Graham CH. Inhibition of human trophoblast invasiveness by high glucose concentrations. The Journal of Clinical Endocrinology and Metabolism. 2005; 90: 4846–4851.

[28] Bryson CL, Ioannou GN, Rulyak SJ, Critchlow C. Association between gestational diabetes and pregnancy-induced hypertension. American Journal of Epidemiology. 2003; 158: 1148–1153.

[29] Innes KE, Wimsatt JH. Pregnancy-induced hypertension and insulin resistance: evidence for a connection. Acta Obstetricia Et Gynecologica Scandinavica. 1999; 78: 263–284.

[30] Suhonen L, Teramo K. Hypertension and pre-eclampsia in women with gestational glucose intolerance. Acta Obstetricia Et Gynecologica Scandinavica. 1993; 72: 269–272.

[31] Garner PR, D'Alton ME, Dudley DK, Huard P, Hardie M. Preeclampsia in diabetic pregnancies. American Journal of Obstetrics and Gynecology. 1990; 163: 505–508.

[32] Bateman AR, Bateman GA, Barber T. The relationship between cerebral blood flow and venous sinus pressure: can hyperemia induce idiopathic intracranial hypertension? Fluids and Barriers of the CNS. 2021; 18: 5.

[33] Elshennawy A. Effect of Gestational Diabetes on Gross Morphology, Histology and Histochemistry of Human Placenta. Endocrinology & Metabolic Syndrome. 2016; 5: 1–13.

[34] Sáez T, de Vos P, Sobrevia L, Faas MM. Is there a role for exosomes in foetoplacental endothelial dysfunction in gestational diabetes mellitus? Placenta. 2018; 61: 48–54.

[35] Aires MB, Dos Santos ACV. Effects of maternal diabetes on trophoblast cells. World Journal of Diabetes. 2015; 6: 338–344.

[36] Sánchez-Santos A, Martínez-Hernández MG, Contreras-Ramos A, Ortega-Camarillo C, Baiza-Gutman LA. Hyperglycemia-induced mouse trophoblast spreading is mediated by reactive oxygen species. Molecular Reproduction and Development. 2018; 85: 303–315.

[37] Jarmuzek P, Wielgos M, Bomba-Opon D. Placental pathologic changes in gestational diabetes mellitus. Neuro Endocrinology Letters. 2015; 36: 101–105.

[38] Cvitic S, Desoye G, Hiden U. Glucose, insulin, and oxygen interplay in placental hypervascularisation in diabetes mellitus. BioMed Research International. 2016; 2014: 145846.
[39] Gewolb IH, Merdian W, Warshaw JB, Enders AC. Fine structural abnormalities of the placenta in diabetic rats. Diabetes. 1986; 35: 1254–1261.
[40] Farias PS, dos S Souza K, Fioretto ET, dos Santos MRV, Aires MB. Maternal diabetes affects rat placental morphology and pregnancy. Endocrine. 2014; 45: 497–501.
[41] Ne'eman Z, Barash V, Rosenmann E, Shafrir E. Localization of glycogen in the placenta of diabetic rats: a light and electron microscopic study. Placenta. 1987; 8: 201–208.
[42] Prager R, Abramovici A, Liban E, Laron Z. Histopathological changes in the placenta of streptozotocin induced diabetic rats. Diabetologia. 1974; 10: 89–91.
[43] Wong SF, Chan FY, Oats JJN, McIntyre DH. Fetal growth spurt and pregestational diabetic pregnancy. Diabetes Care. 2002; 25: 1681–1684.
[44] Becerra JE, Khoury MJ, Cordero JF, Erickson JD. Diabetes mellitus during pregnancy and the risks for specific birth defects: a population-based case-control study. Pediatrics. 1990; 85: 1–9.
[45] Hendricks KA, Nuno OM, Suarez L, Larsen R. Effects of hyperinsulinemia and obesity on risk of neural tube defects among Mexican Americans. Epidemiology. 2001; 12: 630–635.
[46] Parnell AS, Correa A, Reece EA. Pre-pregnancy Obesity as a Modifier of Gestational Diabetes and Birth Defects Associations: a Systematic Review. Maternal and Child Health Journal. 2017; 21: 1105–1120.
[47] Erickson JD. Risk factors for birth defects: data from the Atlanta Birth Defects Case-Control Study. Teratology. 1991; 43: 41–51.
[48] Lisowski LA, Verheijen PM, Copel JA, Kleinman CS, Wassink S, Visser GHA, *et al*. Congenital heart disease in pregnancies complicated by maternal diabetes mellitus. an international clinical collaboration, literature review, and meta-analysis. Herz. 2010; 35: 19–26.
[49] Lin X, Yang P, Reece EA, Yang P. Pregestational type 2 diabetes mellitus induces cardiac hypertrophy in the murine embryo through cardiac remodeling and fibrosis. American Journal of Obstetrics and Gynecology. 2017; 217: 216.e1–216.e13.
[50] Burton GJ, Fowden AL. The placenta: a multifaceted, transient organ. Philosophical Transactions of the Royal Society B: Biological Sciences. 2015; 370: 20140066.

Supplementary material: Supplementary material associated with this article can be found, in the online version, at https://www.fbscience.com/Landmark/articles/10.52586/5001.

Abbreviations: GDM, gestational diabetes; PGDM, pregestational diabetes; STZ, streptozotocin; JZ, junctional zone; LZ, labyrinth; DZ, decidua; PAS, periodic acid–Schiff; GlyT, glycogen trophoblast; SpT, spongiotrophoblast; SpA, Spiral Artery; VSMC, vascular smooth muscle cell; TGC, trophoblast giant cell; LD, lumen diameter; OD, outer diameter; FCA, fetal capillary area; MLA, maternal lacune area; IHM, interhemal membrane; NTD, neural tube defect; IVS, interventricular septum.

Keywords: Gestational diabetes; Placenta; Spiral artery; Angiogenesis; Birth defects

Send correspondence to: Linglin Xie, Department of Nutrition, Texas A&M University, College Station, TX 77843, USA, E-mail: Linglin.xie@tamu.edu
† These authors contributed equally.
§Current address: Department of Colorectal Surgery, The Sixth Affiliated Hospital of Sun Yat-sen University (Gastrointestinal and Anal Hospital of Sun Yat-sen Unversity), 510655 Guangzhou, Guangdong, China